Iranian Journal of Chemical Engineering
Vol. 14, No. 3 (Summer 2017), IAChE

Methanol Crossover and Selectivity of Nafion/Heteropolyacid/Montmorillonite Nanocomposite Proton Exchange Membranes for DMFC Applications

M. Azimi, S. J. Peighambardoust [*]

Faculty of Chemical and Petroleum Engineering, University of Tabriz, P. O. Box: 51666-16471, Tabriz, Iran

ARTICLE INFO

Article history:
Received: 2016-08-31
Accepted: 2016-10-16

Keywords:
Nafion
Heteropolyacid
Montmorillonite
Proton Exchange Membrane
Methanol Crossover
Selectivity
Direct Methanol Fuel Cell

ABSTRACT

In this work, we prepared the nafion/montmorillonite/heteropolyacid nanocomposite membranes for direct methanol fuel cells (DMFCs). The analyses, such as X-ray diffraction (XRD), Fourier transform infrared (FTIR), and scanning electron microscopy (SEM), were conducted to characterize the filler dispersion and membrane structure in prepared nanocomposite membranes. XRD patterns of nafion-CsPW-MMT nanocomposites membranes showed the exfoliated structure of membranes by adding MMT and CsPW. SEM-EDXA results showed proper dispersion of nanoparticles in the membrane matrices. Addition of CsPW-MMT to nafion membranes increases water uptake and IEC due to the increase of hydrophilic groups in membranes. The proton conductivity results showed that proton conductivity increases by increasing amount of CsPW and decreasing of clay content in the membrane. Methanol crossover through polymer electrolyte membranes is a critical issue and causes an important reduction of performance in DMFCs. The developed intercalated nafion/CsPW/MMT nanocomposite membranes have successfully improved the membrane barrier properties due to the unique feature of MMT which contributed to the formation of a longer pathway towards methanol across the membrane. The lowest methanol crossover of the developed membranes in this study was 1.651×10^{-6} cm^2s^{-1} ***Error! Digit expected.****which is lower than re-cast nafion membrane (*2.078×10^{-6} cm^2s^{-1}*). The methanol permeability was significantly reduced by the incorporation of MMT and increased by addition of CsPW in the nafion membrane. Finally, according to the selectivity results, the nafion-MMT-CsPW nanocomposite membrane with MMT mass fraction of 2.5 % and CsPW mass fraction of 8 % shows the best membrane selectivity and this nanocomposite membrane could be suitable for application in DMFCs.*

1. Introduction

A fuel cell is a device that converts the chemical energy from a fuel into electricity

[*]Corresponding author: j.peighambardoust@tabrizu.ac.ir

through a chemical reaction of positively charged hydrogen ions with oxygen or another oxidizing agent. Proton exchange membrane fuel cells (PEMFCs) are considered to be a promising technology for clean and efficient power generation in the twenty-first century. Direct methanol fuel cells (DMFCs) have great potential in generating electricity owing to their high efficiency and lightness. However, two major technical limitations restrict the commercialization of the DMFC. They are the slow oxidation kinetics of methanol and the high methanol crossover from the anode to the cathode [1]. Perfluorosulfonic acid (PFSA) group membranes, such as nafion, have been commercially used in hydrogen-oxygen fuel cell applications to serve as an electrolyte. Due to its good conductivity and good thermal stability, its use has been established in DMFC and PEMFC [2]. However, nafion faces several drawbacks which limit its industrial applications. One of the disadvantages is the high production cost, which is 700 US $ m^{-2} [3]. Furthermore, it has low-proton conductivity at high temperatures because of fast dehydration and loss of fluorine ion in the exhaust gas due to OH radical attack [4]. Besides, the key problem for nafion use in DMFC is the high-methanol crossover which allows for methanol diffusivity of 1.0×10^{-6} cm^2s^{-1} even at room temperature [5]. For the past 20 years, polymer-clay nanocomposites have attracted much attention both academically and industrially [6]. Great studies have been conducted by incorporating polymer with clay and the result showed that clay was a methanol barrier. This discovery was proven by the decrease in methanol permeability of the nanocomposite membranes as compared to pristine based polymer [7]. However, the addition of clay into polymer reduces its proton conductivity which is not favorable in DMFC application [8]. Thus, several attempts have been made to reduce methanol permeability without sacrificing too much proton conductivity by using silane agent [9], grafting sulfonic group into silicate layer [10, 11], or by organically modifying the clay using quaternary ammonium salt [12-14], etc. The ionic cluster of hydrophilic polymer backbone is obstructed by the inorganic filler, which disturbs the proton transportation within the hydrophilic channels. Although clay is known as a proton conductor, the value of 1×10^{-4} Scm^{-1} is not high enough to maintain good proton conductivity in polymer/clay nanocomposite membranes. Another approach to increase the proton conductivity of the clay without destroying its silicate layers is by mixing heteropolyacid (HPA) with clay to increase its proton conductivity [13]. In this paper we mixed cesium salt of heteropolyacids with MMT to increase nanocomposite membranes' proton conductivity.

2. Experimental

2.1. Materials

N,N-Dimethylformamide, tungstophosphoric acid hydrate and cesium carbonate were supplied by Merck. DuPont supplied Nafion-117 resins and Aldrich supplied MMT K10 clay filler. They were used as received without further purification.

2.2. Preparation of cesium hydrogen salt of HPAs (CsPW)

Cesium salt of heteropolyacids (hereafter, CsHPs), including CsPW, was prepared by precipitation titration. The aqueous solutions of tungstophosphoric acid (0.08 M) and Cs_2CO_3 (0.1 M) were prepared. Cs_2CO_3

solution was added to 20 mL of HPA solution dropwise with stirring in room temperature. The colloidal solution was stirred overnight, and then liquid phase was evaporated at 45 °C. The powders of CsPW were obtained by heating at 300 °C for 1 h. Finally, the prepared powders were grinded and stored in a dry atmosphere before use.

2.3. Preparation of the Nafion/MMT/CsPW nanocomposite membrane

Nanocomposite membranes were prepared by recast procedure. The nafion resins were solved in DMF under 90 °C to reach mass fraction of 5 % nafion solution. CsPW and MMT (specific mass fraction % based on solid nafion) were dispersed in DMF with stirring to avoid particle aggregation mixed for 24 h. Then, they were added to nafion with mass fraction of 5 % solution and sonicated for 30 minutes. The concentrated and viscous solution was poured into a Petri dish. Membranes were dried preliminarily at 45 °C for 42 h. The solvent evaporated completely at 50 °C (24 h). Dried membranes were peeled off from the surface and their organic and inorganic impurities were removed by boiling in 3 % H_2O_2 (w/v) for 180 min. Membranes boiled in H_2SO_4 0.5 M for 180 min for protonation and washed in boiling deionized water for 30 min. Membranes boiled in HNO_3 for 180 minutes, and finally washed in boiling deionized water for 30 min. Recast nafion membranes without inorganic filler were also prepared by the same procedure. The thickness of the nanocomposite membranes was controlled by mild membrane drying and measured by a digital micrometer provided by Mitutoyo. The average thickness of the whole prepared membrane samples is 45±5 μm. Table 1 summarizes different types of nafion/MMT/CsPW nanocomposites in terms of clay and heteropolyacid contents.

Table 1
Different types of nafion/MMT/CsPW nanocomposites in terms of clay and heteropolyacid contents.

Membrane code	Montmorillonite wt %	$Cs_{2.5}H_{0.5}PW_{12}O_{40}$ wt %	Nafion-117 wt %
1 (Pure Nafion)	0	0	100
2	2.5	0	97.5
3	5	0	95
4	0	8	92
5	0	16	84
6	1.25	12	86.75
7	2.5	8	89.5
8	3.75	4	92.25

3. Characterization methods

3.1. Fourier transform infrared (FT-IR) analysis

FTIR spectra of primary heteropolyacid ($H_3PW_{12}O_{40}$) and cesium salt of this HPA ($Cs_{2.5}H_{0.5}PW_{12}O_{40}$) were recorded on a Bruker Tensor 27 spectrometer. The KBr pellet method was used to measure the spectra powder samples.

3.2. Membrane structure characterization by X-ray diffraction (XRD) analysis

To study the structure of the prepared nanocomposite membranes and dispersing phase arrangement, X-ray diffraction analysis was used. XRD analysis was performed at 25 °C using a Siemens powder diffractometer with Cu-Kα radiation (λ=1.5406 Å) in the center of the Geological Survey of Iran (Tabriz). XRD patterns were obtained in 2θ = 2-10° with step size of 0.02°/min. Operating current and voltage were 30 mA and 60 kV, respectively. This analysis has been used for quantitative calculation of the distance between the plates of clay silicates by using Bragg's law in nanocomposites and pure clay mineral powder.

3.3. Scanning electron microscopy (SEM) analysis

The morphology of the nanocomposite membranes' cross-section was investigated by scanning electron microscopy (SEM). Nanocomposite membrane specimen for the SEM observations was prepared by freezing the dry membrane sample in liquid nitrogen up to 10 min and breaking it to produce a fresh cross-section. Fresh cross-sectional cryogenic fractures of the film ware vacuum sputtered with a thin layer of gold (Au) using an ion sputtering before observing the scanning electron microscope (VEGA\\TESCAN, Czech Republic) with a potential of 300 V to 20 kV. To determine the MMT and HPA nanoparticles' distribution along the nanocomposite membranes in cross-section of these films, the elemental profiles across the sample thicknesses were obtained by energy dispersive X-ray analysis (EDXA) by Oxford Instruments Microanalysis model 7718 INCA PentaFET.

3.4. Water uptake measurements

Water uptake (WU) of membranes at room temperature was calculated by taking the difference between the wet and dry weights of nanocomposite membrane samples. Nanocomposite membranes with different amounts of MMT and CsPW were equilibrated with deionized water at 50 °C in 6 h. The samples were then removed, dried with tissue papers, and then weighed. The dry weights of membranes were also measured after vacuum drying of the samples at 100 °C for 24 h. The water uptake of all membrane samples was calculated from the following equation:

$$\text{Water Uptake (\%)} = \frac{W_{Wet} - W_{Dry}}{W_{Dry}} \times 100 \quad (1)$$

where W_{Wet} is the membrane weight after cleaning and when the surface water was removed and W_{Dry} is the membrane weight after drying at 100 °C.

3.5. Ion exchange capacity (IEC) measurements

The ion exchange capacity (IEC) is defined as mequivalents of $-SO_3H$ groups per gram of dry membrane. To measure the IEC of the nanocomposite membrane samples, they were immersed in a 1.0M NaCl solution for 24 h. The released H^+ ions due to the ion exchange reaction with Na^+ ions were back titrated with a 0.1 M NaOH solution, in which phenolphthalein was added as an indicator. The ion exchange capacity (IEC) of the membranes was calculated by the following equation:

$$IEC = \frac{V_{NaOH}(mL) \times M_{NaOH}(mol\ L^{-1})}{W_{Dry}(gr)} \quad (2)$$

3.6. Proton conductivity measurement

The proton conductivity of different membranes and their nanocomposites was measured by the two electrode AC impedance

method transverse [14]. A sample of the membrane was placed between two copper disc electrodes and proton conductivities of the developed membranes were measured by AC impedance spectroscopy over three different frequency ranges of 1, 5 and 10 Hz. The most crucial step prior to proton conductivity measurements is that nanocomposite membrane samples must be soaked in water at room temperature for hydration. The thickness of the hydrated membranes was then measured by micrometer several times to obtain the average membrane thickness. The conductivity (in S cm^{-1}) of samples in the transverse direction is calculated as follows:

$$\sigma = \frac{d}{R_m . S} \quad (3)$$

where d and S are the thickness (in cm) and the surface area (in cm^2) of the membrane sample, respectively, and R_m (in ohm) is the resistance of membrane. Figure 1 shows the schema of the system used to determine resistance of nanocomposite membranes.

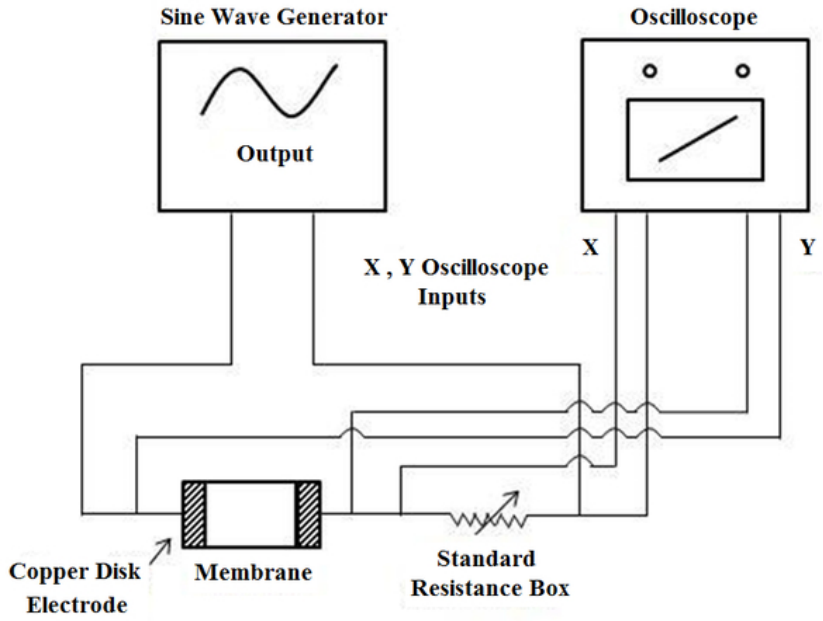

Figure 1. Schema of the used system to determine resistance of nanocomposite membranes.

3.7. Methanol permeability measurements

Methanol permeability measurements were conducted by using a diffusion cell, as shown in figures 2 (a,b). The cell was divided into two compartments, in which one compartment was filled with deionized water (called B compartment) and the other compartment was filled with a 2 M CH_3OH aqueous solution (called A compartment). Prior to test, the nafion/CsPW/MMT nanocomposite membrane was hydrated in deionized water for at least 24 h. The nafion/CsPW/MMT nanocomposite membrane with a surface area of 0.7845 cm^2 was sandwiched by O-ring and clamped tightly at between two compartments. The diffusion cell was kept stirring during the experiment. The concentration of alcohol diffused from compartments A to B across the nafion/CsPw/MMT nanocomposite membrane was examined with time by refractive index method using the ATAGO's Abbe Refractometer. The amount of 5 mL was sampled from B compartment every 30 min. Prior to the permeation experiment, the calibration curve for the value of refractive

index vs. the methanol concentration was prepared. The calibration curve was used to calculate the methanol concentration in the permeation experiment.

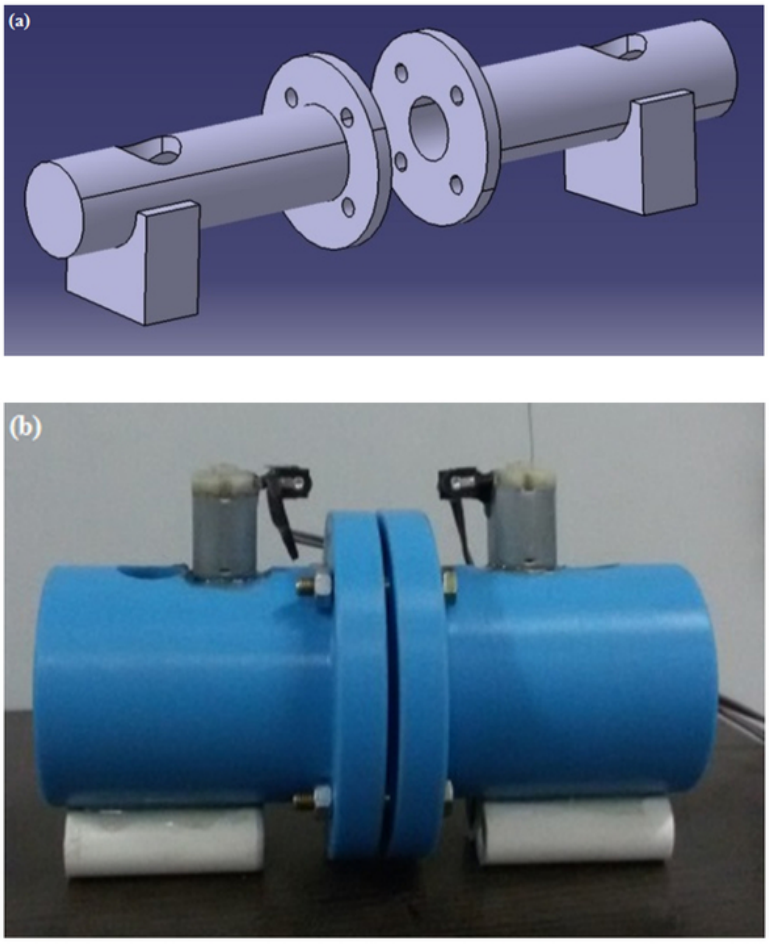

Figure 2. a) Schema of diffusion cell used in methanol permeability test; b) Diffusion cell used in methanol permeability test.

The methanol permeability was calculated from the slope of the straight-line plot of alcohol concentration vs. permeation time. The methanol concentration in B compartment as a function of time is given in the following equation [20]:

$$C_B(t) = \frac{A}{V}\frac{DK}{L}C_A(t - t_0) \quad (4)$$

$$C_B(t) = \frac{A}{V}\frac{DK}{L}C_A(t\text{-}t_0)(1)$$

where C is the alcohol concentration, V is volume, A and L are the polymer membrane area and thickness, and D and K are the alcohol diffusivity and partition coefficient between the membrane and solution. The product D.K is the membrane permeability (P), and t_0 is also termed time lag, related to the diffusivity: $t_0=L^2/6D$. With the above equations and calculation of concentration-time line slope in B compartment, the methanol crossover through membrane was obtained by the following equation:

$$m = \frac{P \cdot A \cdot C_A}{V \cdot L} \quad (5)$$

4. Results and discussion

4.1. Fourier transform infrared (FT-IR) analysis

The FT-IR measurement of primary heteropolyacid ($H_3PW_{12}O_{40}$) and the prepared CsPW heteropolyacid salt are represented in

Figure 3. It was found that there is a Keggin structure in heteropolyacid materials. The 12-tungstophosphoric acid with Keggin structure has layered network structure made of WO_6 octahedral and PO_4 tetrahedral. Therefore, there are four types of oxygen atoms in Keggin structure of these heteropolyacid materials observed as P-O bond in PO_4 tetrahedrals: W-O_c-W and W-O_e-W bonds in WO_6 octahedrals and W=O bond.

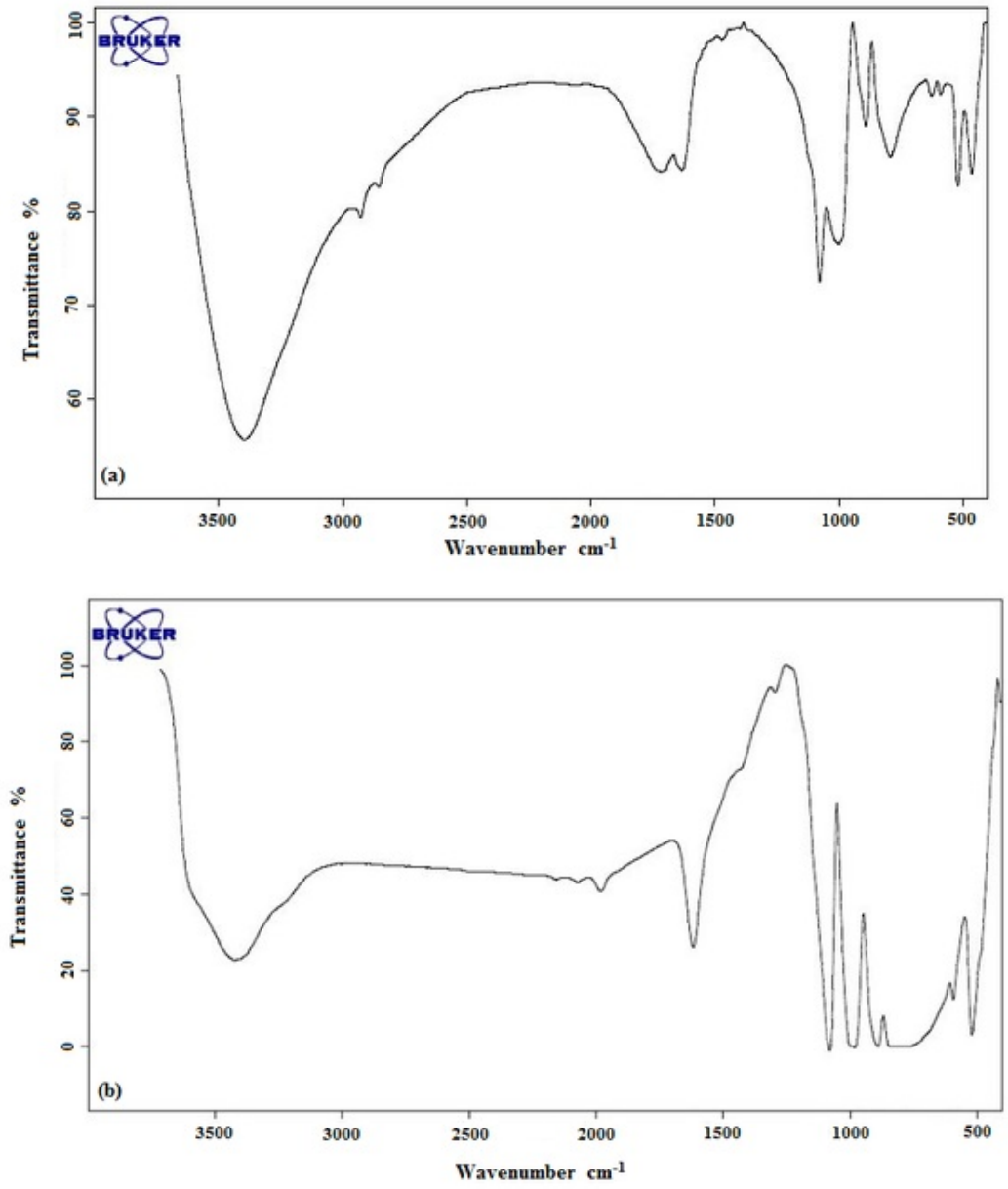

Figure 3. FTIR spectra of a) Primary heteropolyacid ($H_3PW_{12}O_{40}$) and b) Cesium salt of this heteropolyacid ($Cs_{2.5}H_{0.5}PW_{12}O_{40}$).

From figure 3a, typical characteristic peaks at wave numbers of 793 cm^{-1}, 891 cm^{-1}, 1,001 cm^{-1} and 1,078 cm^{-1} are related to the vibrations of four types of oxygen atoms in Keggin structure of heteropolyacid. The absorption peak in wave number of 793 cm^{-1} is attributed to the asymmetric vibrations of W-O_e-W bond, absorption peak at 891 cm^{-1} is related to the asymmetric vibrations of W-O_c-W bond, absorption peak at 1,001 cm^{-1} is related to the vibrations of W=O bond in terminal oxygen attached to Keggin structure

and absorption peak at 1,078 cm^{-1} is related to the vibrations of P=O bond in central tetrahedral of Keggin structure of heteropolyacid. Also, the observed absorption peak at 3,397 cm^{-1} is related to the vibrations of O-H bond of crystallization eater in heteropolyacid structure. By investigating FTIR spectra of primary heteropolyacid ($H_3PW_{12}O_{40}$) and $Cs_{2.5}H_{0.5}PW_{12}O_{40}$ in figure 3b, it can be observed that absorption peaks related to four types of oxygen atoms of Keggin structure of primary heteropolyacid were observed in $Cs_{2.5}H_{0.5}PW_{12}O_{40}$ spectrum, and the whole spectrum was found to be in good agreement with the results available in the literature [15]. The main bands are assigned. The primary Keggin structure (PWA) remains unaltered in the cesium salt forms. For CsPW, the bands at 1,078, 981, 890, 784 and 588 cm^{-1} are assigned to stretching vibrations of P–O, W=O, W–O_c–W corners shared bonds, W–O_e–W edges shared bonds and to the bending vibration of O–P–O, respectively. Absorption band at 1,617 indicates the presence of water ion ($H_5O_2^+$) in the structure of CsHPs and is assigned to $\delta(H_2O)$ vibration. The changes in the frequency characteristics of W–O–W edge and $\delta(H_2O)$ in CsPW may be assigned to the interaction between $[PW_{12}O_{40}]^{3-}$ anion and Cs^+ cation.

4.2. X-ray diffraction (XRD) analysis

XRD measures the degree of particles dispersion by estimating the distance between individual platelets after mixing with polymer. Also, XRD studies revealed formation of the intercalated or exfoliated structure in the prepared nanocomposites. Appearance of clay interlayers diffraction sharp peak in the nanocomposite XRD pattern at 2θ angles lower than pristine MMT suggests an increase in the interlayer spacing or gallery of the clay, which is referred to as an intercalated structure prepared nanocomposite. Broadening the peak is considered to be the result of partial exfoliation in the prepared nanocomposite's structure. Finally, when the peak corresponding to the clay interlayer diffraction peak is not observed in the polymer/clay diffractograms, it indicates that enough polymer chains are inserted into the silicate galleries giving rise to the formation of a nanocomposite with an exfoliated structure in which the polymer is nanoscopically confined. Figure 4 shows the XRD patterns of pristine montmorillonite and four types of nafion/MMT/CsPW nanocomposites. As seen in patterns of figure 4c, the peak appeared at 6.86° on the 2θ axis is the diffraction peak from (001) planes in pristine MMT, which is equal to 1.29 nm basal spacing according to the Bragg's law.

As it can be seen in the patterns of figure 4d and 4e, for the nafion-MMT nanocomposite samples with MMT mass fractions of 2.5 and 5 %, this peak due to (001) planes is broadened and shifted toward lower 2θ angles, which means that the slightly increasing of basal spacing is available and the partially exfoliation structure of the prepared nanocomposite has been created. In this structure type, the interlayers of clay are fully opened from each other and well dispersed into polymer matrices. The broad peaks for nafion/MMT nanocomposite membranes observed in 5.26 and 4.81° on the 2θ axis and the basal spacing according to the Bragg's law are equal to 1.67 and 1.83 nm, respectively. In patterns of figures 4a and 4b, the peak corresponding to the clay interlayer diffraction peak is not observed, indicating the formation of a nanocomposite with an

exfoliated structure. Also, from XRD patterns of nafion/MMT/CsPW nanocomposites, the existence of heteropolyacid in nanocomposite matrices dose not affect the exfoliated or intercalated types of nanocomposite structure.

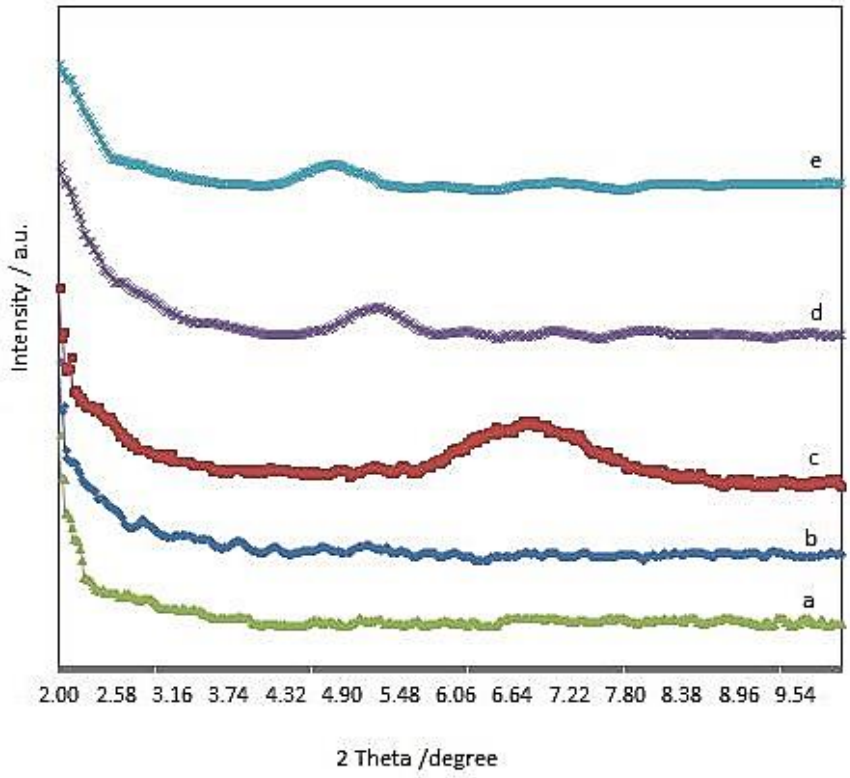

Figure 4. XRD patterns of a) Nafion-1.25 % MMT-12 % CsPW nanocomposite, b) Nafion-2.5 % MMT-8 % CsPW nanocomposite, c) Pristine montmorillonite, d) Nafion-2.5 % MMT nanocomposite and e) Nafion-5 % MMT nanocomposite.

4.3. Scanning electron microscopy (SEM) analysis

In order to investigate the cross-sectional morphology of the prepared nanocomposite membranes and quality of clay and heteropolyacid dispersion into nafion matrices, SEM-EDXA measurements were conducted and the morphology of these membranes is shown in figure 5. In this figure, the SEM images of pure re-cast nafion, nafion-2.5 % MMT, nafion-8 % CsPW and nafion-2.5 % MMT-8 % CsPW nanocomposites are given. The cross-section of the re-cast nafion membrane reveals the dense and homogenous structure of membrane matrix, whereas the cross-sections of nanocomposite membranes with MMT, CsPW and MMT+CsPW represent a rough morphology. The whole membrane cross-section was observed at 20 kx magnification (20000), which does not indicate segregation of different particles and polymeric matrix phase in nanocomposite membranes. It means that the interfacial adhesion and compatibility between polymeric and inorganic phases are suitable in this amount of clay and heteropolyacid in nanocomposite membranes, and there is a no aggregation of nanosized particles in observed morphology for these membranes. Also, the EDXA and dot-mapping of SEM images for one of the nanocomposite membranes is performed and the distribution of different elements into polymer matrices is shown in figure 5e. The

elemental analyses of silicon (Si) and tungsten (W) on the cross-section of the membrane can facilitate better estimation of distribution of MMT and CsPW particles in the nanocomposite membrane. Green dots in this image show the tungsten and red dots show the silicon in the nanocomposite membrane. Figure 5e shows that the tungsten and silicon elements have a very uniform distribution along the cross- section of the nafion-MMT-CsPW nanocomposite membrane, which indicates a good distribution of these particles in this nanocomposite membrane. This implies that MMT and CsPW particles are not recrystallized into large particles after incorporating with nafion resin, but are highly dispersed throughout the polymer matrix.

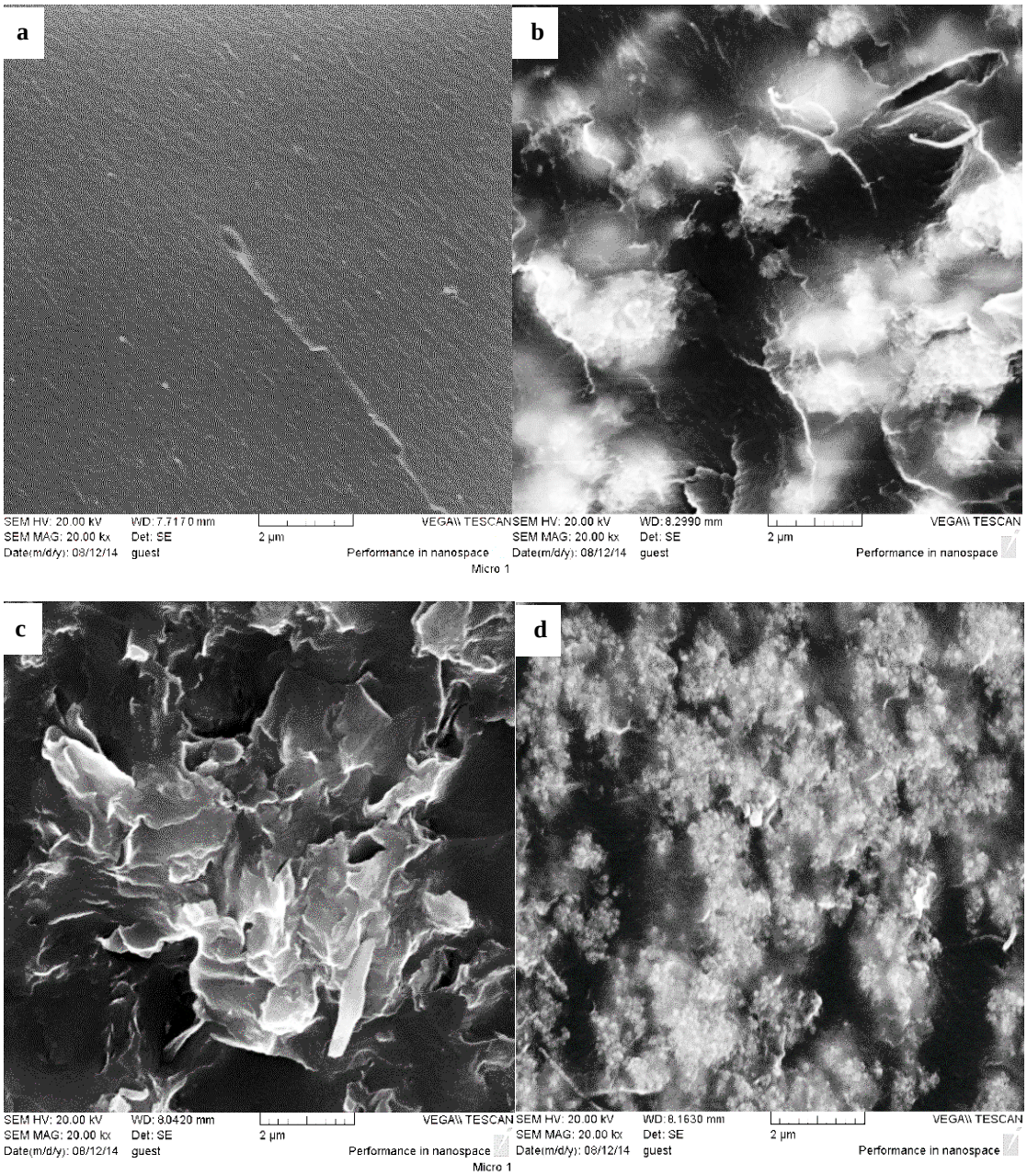

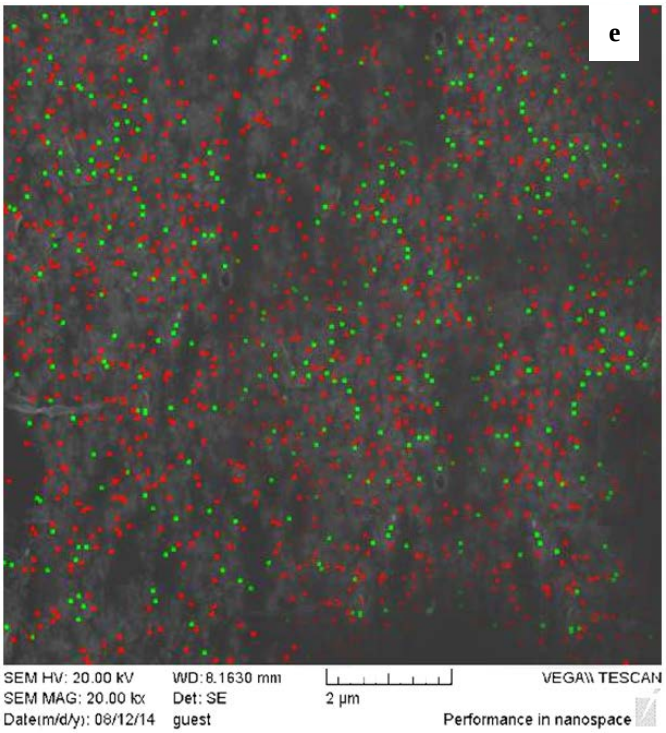

Figure 5. SEM and EDXA analyses of a) Pure re-cast nafion, b) Nafion-2.5 % MMT nanocomposite, c) Nafion-8 % CsPW nanocomposite, d) Nafion-2.5 % MMT-8 % CsPW nanocomposite and e) Dot-mapping of nafion-2.5 % MMT-8 % CsPW nanocomposite (green dots for W element and red dots for Si element).

4.4. Water uptake measurements

To verify the effect of clay and heteropolyacid particles on improving the nanocomposite membrane hygroscopic property, water uptake measurement was conducted for the prepared nanocomposite membranes. The water uptake of the prepared membranes is calculated by equation (1), represented in table 2. As seen in table 2, by increasing the mass fraction of CsPW up to 16 %, water uptake of nanocomposite membrane increases 68 % because water molecules in the secondary structures connect the individual heteropolyanions through weak hydrogen bonds. In the case of $[PW_{12}O_{40}]^{3-}$, its radius is only 0.5-0.6 nm, while the spacing between ions is 23 nm, leaving therefore a considerable space between ions. This space may hold water and increase water content through the nanocomposite membrane. The particle and crystallite sizes of CsHP are not smaller than nafion clusters to make an embedded type of nanocomposite and these particles may settle on the clusters and shield the nafion sulfonic groups. Therefore, although the addition of inorganic CsHP to nafion matrix enhances the water contents, it may limit the activity of hydrophilic sulfonic group of the nafion cluster. On the other hand, by increasing the amount of MMT in membranes, water uptake increases about 25 %. This behavior is clearly explained by the hydrophilic nature of the clay mineral. The nanocomposite membranes, containing both MMT and CsPW, have more water uptake than membranes with only MMT and less water uptake than membranes with only CsPW because CsPW has more hydrophilic groups than MMT. In hydrated phase, Keggin ions of CsPW tend to create molecular bridges with other Keggin ions in the presence of hydronium ions in water.

Table 2
Water uptake measurements of different nanocomposite membranes.

Membrane code	Montmorillonite wt %	$Cs_{2.5}H_{0.5}PW_{12}O_{40}$ wt %	Water uptake %
1 (Pure Nafion)	0	0	36.12
2	2.5	0	41.76
3	5	0	45.34
4	0	8	51.32
5	0	16	68.08
6	1.25	12	53.04
7	2.5	8	62.41
8	3.75	4	49.73

The forming of the hydronium ion bridges allows the CsPW to retain more water in the nanocomposite membranes, which results in higher water uptake. The presence of MMT also helps to increase the water uptake in the membranes. MMT is known as hydrophilic material as the monovalent ions located between the silicates layers tend to attract polar solvent such as water. So, the water uptake of nanocomposite membranes is associated with two factors including sulfonic group of nafion and hygroscopic nature of CsHP and MMT nanoclusters [6,19]. The nafion-MMT-CsPW nanocomposite membrane with mass fraction of 2.5 % MMT and 8% CsPW shows the best water uptake of nanocomposite membrane.

4.5. Ion exchange capacity (IEC) measurements

Ion exchange capacity (IEC) provides an indirect, yet reliable, approximation of the proton conductivity. IEC provides an indication of the content of sulfonic acid groups in the membrane. IEC measurements of plain nafion and nanocomposites were calculated by equation (2) and are shown in table 3. As seen in table 3, by increasing the only clay content into nanocomposite membrane, the IEC of nanocomposite membranes is lower than the plain nafion. This effect is due to covering the nafion active sites (sulfonic groups) and decreasing the effective number of replaceable ion exchange sites by fillers [13,6]. Also, by increasing the heteropolyacid content into nafion matrices of nanocomposite membranes, the IEC firstly increased and then decreased. The main reason for increasing nanocomposites' IEC is due to the hydrophilic nature of heteropolyacid particles and the decrease of nanocomposites' IEC is due to covering the nafion active sites (sulfonic groups) and decreasing the effective number of replaceable ion exchange sites by fillers. The nafion-MMT-CsPW nanocomposite membrane with MMT mass fraction of 2.5 % and CsPW mass fraction of 8 % shows the best IEC of nanocomposite membrane.

Table 3
Ion exchange capacity (IEC) measurements of different nanocomposite membranes.

Membrane code	Montmorillonite wt %	$Cs_{2.5}H_{0.5}PW_{12}O_{40}$ wt %	Ion exchange capacity mequiv./gr
1 (Pure Nafion)	0	0	0.87
2	2.5	0	0.79
3	5	0	0.71
4	0	8	1.26
5	0	16	1.17
6	1.25	12	1.08
7	2.5	8	1.20
8	3.75	4	0.92

4.6. Proton conductivity measurements

Proton conductivity is the most essential requirement to enable membranes to be applicable in DMFC. The proton conductivity of all membranes was measured at 100 % relative humidity. As the test only took few minutes, the water loss from the membranes during measurement was negligible. The membrane resistance and proton conductivity of nafion-MMT-CsPW nanocomposite membranes with different amounts of MMT and CsPW in polymer matrix were calculated by equation (3) and are shown in table 4. According to the results in table 4, by increasing amount of MMT in the nanocomposite membrane, proton conductivity decreases, because the MMT limits movement of polymer matrices chains and also the lower proton conductivity of pristine MMT powder. Also, it was observed that the proton conductivity of nafion-CsPW nanocomposite membranes shows higher proton conductivity values than those of plain nafion membrane because of the proton conductive ability of heteropolyacid present in these membranes. It may be due to the hydrophilic structure of CsPW. These results were consistent with those of water uptake measurements. The increase in proton conductivity of the nafion-CsPW nanocomposite membranes compared to that of plain nafion membrane is ascribed to the combined result of the enhanced water uptake as well as the additional acidity sites provided by CsPW particles. These catalytic proton conductor particles adsorb water to generate the Brönsted acid site for proton transport in nanocomposite membranes. Furthermore, the CsPW particles in the nafion-CsPW nanocomposite membranes can provide additional strong acid group for proton transport and bridge neighboring shrunken clusters to effectively shorten the distance of proton hopping transport, and thus increase the membrane proton conductivity by the Grotthus mechanism. In other words, CsPW particle not only transfers proton by its strong acidity, but also assists sulfonic acid group of the nafion to transfer proton. It can be concluded that the incorporation of CsPW particles increases the acidity and the water uptake of the membrane and thus increases the proton conductivity. In nanocomposite membranes with both MMT and CsPW into nafion matrices, the best proton conductivity belongs to the membrane with lower amount of MMT and higher amount of CsPW (nafion-2.5 % mass fraction MMT-8 % mass

fraction CsPW). Because of low amount of MMT, polymer channels are not limited and protons transfer easily. On the other hand, high amount of CsPW helps to reserve more water in the membrane; therefore, proton conductivity increases.

Table 4
Proton conductivity of different nanocomposite membranes.

Membrane code	Montmorillonite wt %	$Cs_{2.5}H_{0.5}PW_{12}O_{40}$ wt %	Proton conductivity $mS.cm^{-1}$
1 (Pure Nafion)	0	0	2.48
2	2.5	0	2.10
3	5	0	1.95
4	0	8	3.01
5	0	16	3.91
6	1.25	12	3.39
7	2.5	8	3.71
8	3.75	4	2.74

4.7. Methanol crossover and membrane selectivity measurements

Methanol permeation through the ion exchange membrane plays an important role in the performance of direct methanol fuel cells. In a DMFC system, one of the most requirements of PEMs is low methanol permeability. Methanol crossover through different membranes was estimated using equation (5) and the values are presented in table 5. The observed methanol crossover of plain nafion in this study is 2.078×10^{-6} $cm^2\,s^{-1}$ which is similar to the results reported by S. Mollá et al. [16]. High methanol permeability in nafion is attributed to its larger hydrophilic channels formed by sulfonic acid groups in the hydrated phase [17]. The larger hydrophilic channels in nafion allowed more methanol molecules to migrate through the membrane. It is well known that the introduction of clay with low permeability in a membrane leads to a reduction of the overall membrane methanol crossover.

Table 5
Methanol crossover and membrane selectivity measurements of different nanocomposite membranes.

Membrane code	Montmorillonite wt %	$Cs_{2.5}H_{0.5}PW_{12}O_{40}$ wt %	Methanol crossover $\times10^{-7}$ $cm^2.s^{-1}$	Membrane selectivity $\times10^3$
1 (Pure Nafion)	0	0	20.78	1193
2	2.5	0	16.09	1305
3	5	0	13.52	1442
4	0	8	17.75	1696
5	0	16	20.45	1912
6	1.25	12	19.25	1761
7	2.5	8	16.51	2247
8	3.75	4	16.83	1628

The presence of MMT can improve the barrier property of the membrane to methanol molecules. This is likely due to the tortuousness of layered silicate and the lower aspect ratio of the particles resulting from their exfoliation and more tortuous methanol diffusion paths through the nanocomposite membrane. The nafion-MMT and nafion-CsPW-MMT nanocomposite membranes have lower methanol permeability than nafion membrane due to the presence of MMT, which affects the microstructure of hydrophilic domain and obstructs the connected hydrophilic channels, resulting in lower methanol crossover through a longer diffusive pathway [18]. This result differs from the water uptake trend. The introduction of CsPW particles with higher water absorption into membrane at lower content leads to an slight increase of the methanol crossover. However, when the CsPW content into nanocomposite membrane was increased. The methanol crossover of nanocomposite membranes raised due to the increase of hydrophilic groups into membrane structure, but this methanol crossover is still lower than plain nafion. The hydrophilic CsPW is responsible for high methanol permeability, as the hydrophobic matrix hinders excessive swelling. The methanol permeability towards water and methanol depends on the solubility of the membrane. The amount of free water correlates closely with swelling in a methanol aqueous solution [19]. Also, methanol molecules have high affinity with water molecules. Therefore, the methanol permeability of nafion-CsPW increased with the increase of the CsPW content. For DMFC application, the membrane was required to possess high proton conductivity and low methanol crossover. To directly compare the applicability of the prepared PEMs for DMFC applications, the efficiency for separating two components is usually evaluated by selectivity. The membrane selectivity parameter is defined as the ratio of proton conductivity to methanol crossover of membrane. The higher membrane selectivity value leads to a better DMFC membrane performance. This parameter was calculated for different nanocomposite membranes with various CsPW and MMT loadings and is shown in table 5. The nafion-MMT-CsPW nanocomposite membrane with 2.5 % mass fraction of MMT and 8 % mass fraction of CsPW shows the best membrane selectivity mainly due to its decreased methanol permeability and similar increased proton conductivity. The results suggest that this nanocomposite membrane may be suitable for application in DMFCs [20-23].

5. Conclusions

The nafion-based nanocomposite membranes with CsPW particles mixed with MMT membranes were prepared and characterized. XRD patterns of nafion-CsPW-MMT nanocomposites membranes showed the exfoliated structure of membranes by adding amount of MMT and CsPW. SEM-EDXA results showed proper dispersion of nanoparticles in the membrane matrices. Addition of CsPW-MMT to nafion membranes increases water uptake and IEC due to the increase of hydrophilic groups in membranes. The proton conductivity results showed that proton conductivity increases by the increasing amount of CsPW and decreasing amount of clay content in the membrane. The developed intercalated nafion/CsPW/MMT nanocomposite membranes have successfully improved the membrane barrier properties due to the unique

feature of MMT, which contributed to the formation of a longer pathway towards methanol across the membrane. The methanol crossover was significantly reduced by the incorporation of MMT and increased by addition of CsPW in the Nafion membrane. Finally, according to the selectivity results, the nafion-MMT-CsPW nanocomposite membrane with 2.5 % mass fraction of MMT and 8 % mass fraction of CsPW shows the best membrane selectivity and this nanocomposite membrane may be suitable for application in DMFCs.

Acknowledgements

The authors are grateful for the financial support of "Iran Nanotechnology Initiative Council" and "Fuel Cell Steering Committee".

References

[1] Mohd Norddin, M. N. A., Ismail, A. F., Rana, D., Matsuura, T. and Tabe, S., "The effect of blending sulfonated poly(ether ether ketone) with various charged surface modifying macromolecules on proton exchange membrane performance", *J. Membr. Sci.*, **328** (1-2), 148 (2009).

[2] Munakata, H., Yamamoto, D. and Kanamura, K., "Three-dimensionally ordered macroporous polyimide composite membrane with controlled pore size for direct methanol fuel cells", *J. Power Sources*, **178** (2), 596 (2008).

[3] Yildirim, M. H., Stamatialis, D. and Wessling, M., "Dimensionally stable nafion–polyethylene composite membranes for direct methanol fuel cell applications", *J. Membr. Sci.*, **321** (2), 364 (2008).

[4] Lufrano, F., Baglio, V., Staiti, P., Arico, A. S. and Antonucci, V., "Polymer electrolytes based on sulfonated polysulfone for direct methanol fuel cells", *J. Power Sources*, **179** (1), 34 (2008).

[5] Zhang, X., Tay, S. W., Hong, L. and Liu, Z., "In situ implantation of PolyPOSS blocks in Nafion® matrix to promote its performance in direct methanol fuel cell", *J. Membr. Sci.*, **320** (1-2), 310 (2008).

[6] Peoples, B. C., "In situ production of polyolefin-clay nanocomposites", Ph. D. dissertation, University of California, (2008).

[7] Hasani-Sadrabadi, M. M., Emami, S. H. and Moaddel, H., "Preparation and characterization of nanocomposite membranes made of poly(2,6-dimethyl-1,4-phenylene oxide) and montmorillonite for direct methanol fuel cells", *J. Power Sources*, **183** (2), 551 (2008).

[8] Fu, T., Cui, Z., Zhong, S., Shi, Y., Zhao, C., Zhang, G., Shao, K., Na, H. and Xing, W., "Sulfonated poly(ether ether ketone)/clay-SO_3H hybrid proton exchange membranes for direct methanol fuel cells", *J. Power Sources*, **185** (1), 32 (2008).

[9] Peighambardoust, S. J., Rowshanzamir, S. and Amjadi, M., "Review of the proton exchange membranes for fuel cell applications", *Int. J. Hydrogen Energy*, **35** (17), 9349 (2010).

[10] Kim, T. K., Kang, M., Choi, Y. S., Kim, H. K., Lee, W., Chang, H. and Seung, D., "Preparation of nafion-sulfonated clay nanocomposite membrane for direct menthol fuel cells via a film coating process", *J. Power Sources*, **165** (1), 1 (2007).

[11] Gaowen, Z. and Zhentou, Z.,

"Organic/inorganic composite membranes for application in DMFC", *J. Membr. Sci.*, **261** (1-2), 107 (2005).

[12] Lee, S. K. Gento, M., Zhuolin, L., Hui, K. S., Sang, K. L., Hui, K. N., Park, S. Y., Ha, Y. J. and Kim, J. W., "Measuring the relative efficiency of hydrogen energy technologies for implementing the hydrogen economy: An integrated fuzzy AHP/DEA approach", *Int. J. Hydrogen Energy*, **36** (20), 12655 (2011).

[13] Peighambardoust, S. J., Rowshanzamir, S., Hosseini, M. G. and Yazadanpour, M., "Self-humidifying nanocomposite membranes based on sulfonated poly(ether ether ketone) and heteropolyacid supported Pt catalyst for fuel cells", *Int. J. Hydrogen Energy*, **36** (17), 10940 (2011).

[14] Jian, T., Peng, G., Zhi, Z., Wen, L. and Zhong, S., "Preparation and performance evaluation of a nafion-TiO_2 composite membrane for PEMFCs", *Int. J. Hydrogen Energy*, **33** (20), 5686 (2008).

[15] Rocchiccioli-Deltcheff, C., Thouvenot, R. and Franck, R., "Spectres i.r. et Raman d'heteropolyanions", *Spectrochimica Acta Part A: Molecular Spectroscopy*, **32** (3), 587 (1976).

[16] Mollá, S., "On the methanol permeability pristine nafion® and nafion/PVA membranes measured by different techniques: A comparison of methodologies", *Fuel Cells*, **11** (6), 897 (2011).

[17] Cui, Z., Xing, W., Liu, C. and Zhang, H., "Chitosan/heteropolyacid composite membranes for direct methanol fuel cell", *Journal of power sources*, **188** (1), 24 (2009).

[18] Müinch, W., Kreuer, K. D., Traub, U. and Maier, J., "Proton transfer in the three-dimensional hydrogen bond network of the high temperature phase of $CsHSO_4$: A molecular dynamic study", *J. Mol. Struct.*, **381** (1-3), 1 (1996).

[19] Corma, A., "Inorganic solid acids and their use in acid-catalyzed hydrocarbon reactions", *Chemical Reviews*, **95**, 559 (1995).

[20] Izumi, Y., Ogawa, M. and Urabe, K., "Alkali metal salts and ammonium salts of Keggin-type heteropolyacids as solid acid catalysts for liquid-phase Friedel-Crafts reactions", *Applied Catalysis A: General*, **132** (1), 127 (1995).

[21] Rozenberg, B. A. and Tenne, R., "Polymer-assisted fabrication of nanoparticles and nanocomposites", *Progress in Polymer Science*, **33** (1), 40 (2008).

[22] De´ka´ny, I. and Haraszti, T. S., "Layered solid particles as self-assembled films", *Colloids and Surfaces A: Physicochemical and Engineering Aspects*, **123**, 391 (1997).

[23] Barbora, L., "A novel composite nafion membrane for direct alcohol fuel cells", *Journal of Membrane Science*, **326** (2), 721 (2009).